

Towards Moving Virtual Arms Using Brain-Computer Interface

Abstract Motor imagery Brain-Computer Interface (MI-BCI) is a paradigm widely used for controlling external devices by imagining bodily movements. This technology has inspired researchers to use it in several applications such as robotic prostheses, games, and virtual reality (VR) scenarios. To the authors' knowledge, nevertheless, embodied BCI has only been used as a neurofeedback training instead as a control command, even though that psychology has conclusively demonstrated the existence of body transfer illusions (rubber hand illusion). Thus, we study the inclusion of an imaginary third arm as a part of the control commands for BCI. Ten healthy subjects participated in a two-session experiment involving open-close hand tasks (including a third arm that comes out from the chest). To validate the proposed paradigm, we used two VR scenarios: the classical BCI Graz, with arrows as feedback; and a first-person view of a human-like avatar performing the corresponding tasks. The EEG analysis shows a strong power decrease in the sensory-motor areas for the third arm task in both scenarios. Furthermore, the offline classification results show that a third arm can be effectively used as a control command (accuracy > 0.62%). Likewise, the human-like avatar condition (67%) outperforms the Graz condition (63%) significantly, suggesting that the realistic scenario can reduce the abstractness of the third arm, however, this condition induces a cognitive load. This study, thus, motivates the further inclusion of non-embodied motor imagery task in BCI systems.

Keywords Brain-Computer Interaction · Virtual Reality · Rubber Hand Illusion

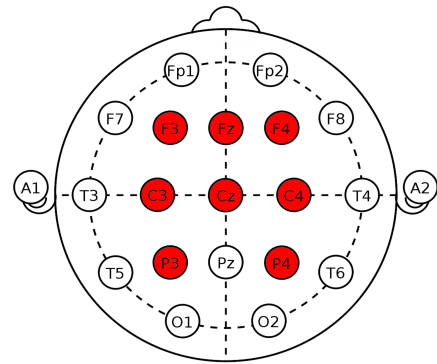


Fig. 1 Experiment setup: A subject using a BCI interface to control his “three” arms in a virtual reality experience (top); and the electrodes placement over the sensorimotor area (filled circle), following the 10-20 system (bottom).

1 Introduction

Along the years, researchers have sought different alternatives to allow human-machine communication. In this context, Brain-Computer Interface (BCI) plays a major role, motivated by overcoming the difficulties experienced by im-

paired people [27] or just by providing a non-mechanical user interface [14]. BCI employs the electrical activity in the brain elicited during a specific task. Depending on the nature of this activity, BCI is characterized as passive, active or reactive [39]. Passive systems use signals that arise without voluntary control. It is used fundamentally to assess mental states and enhance the human-computer interaction [40]. Active BCI works with the self-induced brain activity produced by the user independently of external events. It has been used as a control signal [38]. Finally, reactive BCI relies on the signals elicited by the reaction to specific external stimuli, which could be used to control an application as well [11].

Since the activation patterns of imaginary body movements involve both brain regions (sensory and motor areas) and neural mechanisms similar to the executed movement [17], the Motor Imagery BCI (MI-BCI) has been widely used and explored in active BCI [37]. MI-BCI employs the amplitude changes voluntarily elicited by the mental representation of physical motor actions. Such variations are known as event-related desynchronization and synchronization (ERD/ERS). These patterns have been successfully used for studying the neural mechanisms associated with motor actions, as well as a feature for classification in motor-related BCI systems [14, 27, 33, 37].

So far, MI-BCI applications have used attached body parts, in other words, mental representations of jointed limbs following the human anatomy constraints (e.g., two arms, two legs, two feet, in a symmetrical distribution). To the authors' knowledge, nevertheless, there is neither explorations nor applications that include non-embodied human limbs, although the Rubber Hand Illusion (RHI) experiments demonstrated the human capabilities to create body transfer illusions [6, 12]. Indeed, the RHI not only demonstrates a static body illusion representation (sense of ownership), but also an active movement eliciting a body illusion (sense of agency) [18].

Likewise, despite BCI being a promising and useful application, there are still several challenges to be addressed. Chavarriaga et al. [8] discuss concrete research avenues and guidelines to overcome common pitfalls in BCI. Their paper is the outcome of a meeting held at the workshop "What's wrong with us? Roadblocks and pitfalls in designing BCI applications". They summarize four main topics that influence any closed-loop BCI system: *a)* End Users; *b)* Feedback and user training; *c)* Signal processing and decoding; and *d)* Performance metrics and reporting.

The fast growth of machine learning and unsupervised systems (i.e. deep learning) have supported the signal processing of EEG data and consequently, BCI systems [22]. As BCI is a relatively new research area, establishing metrics to objectively assess BCI systems (e.g., classification accuracy plus usability) is still a task to be done. Potential user

identification is a mandatory step to design suitable BCI applications. However, this requires additional resources and developments of wearable recording equipment. Finally, the training and feedback should consider human factors and include the user inside the BCI loop through a more realistic, natural and intuitive training and feedback.

Recently, immersive technologies have played an essential role in overcoming the training and feedback challenge. Among them, Virtual Reality (VR) is the most promising technology, giving the users a sensation of full immersion in virtual worlds. VR has been effectively used in several areas, from health-care for rehabilitation and training [15] up to data visualization and serious games [10, 13]. Likewise, VR has been used in BCI for a visual feedback presentation of the current task carried out by the user. Lécuyer et al. [25] discuss some of the current applications developed using BCI with VR, namely MindBalance [19], Simulation of wheelchair control [20], and "use the force" [24]. These studies, as highlighted by the author, show the successful use of VR with BCI.

In that vein, this work studies the inclusion of a third arm as a control command in a BCI system. This study was done in two steps: EEG analysis of the induced brain oscillatory activity elicited by the third arm using Event-Related Spectral Perturbation (ERSP) and power changes; and an offline exploration of the classification of the third arm task. In order to explore as much as possible the differences in the classification of this task, several time windows were used in a Filter-Bank Common-Spatial Pattern (FBCSP) [3] for extracting features to train three classifiers: Support Vector Machine (SVM), K-Nearest Neighbors (KNN) and Linear Discriminant Analysis (LDA). Throughout such effort, we compared two training conditions: the traditional Graz paradigm and a realistic human-like feedback. Moreover, we included a cognitive load assessment using both subjective questionnaire (NASA-TLX) [16] and the Task Load Index [36] in the comparison. Finally, we used the Movement Imagery Questionnaire - 3 (MIQ - 3) [26] before the experiment to assess the movement imagery ability of the users in order to find out any correlation related to the classification performance. In light of the results, we argue the feasibility of including the virtual third arm into a BCI system, and in line with the literature, the realistic training enhances the modulation of ERS/ERD patterns, and consequently, the performance of the user in motor imagery tasks.

The rest of the paper is structured as follows: section two presents the state-of-art in BCI, mainly the applications that use either VR or body illusions. Then, section 3 shows the materials, methods, and details of the experimental procedure. Finally, section 4 provides the main findings separated in EEG analysis and classification results; meanwhile, section 5 discusses the findings, and section 6 presents the concluding remarks.

2 Related Works

Virtual Reality is a powerful tool to improve the BCI training and enhancing the feedback experiences [28]. The learning task should include an intuitive feedback so that the user can easily understand the action to be executed and improve its performance. However, it is currently hard to choose the right feedback presentation, and it should be a motivating and engaging environment, as point out [8], besides natural and realistic. Here, VR can be shown as a real alternative for tackling the feedback presentation issue.

Lotte et al. [23] show how combining BCI with VR can carry towards a new and improved BCI system. Nevertheless, such VR feedback can also introduce some interference to the motor imagery-related brain activity used by the BCI because both μ and β bands are reactive in motor imagery and observation of the real movement [33]. An interesting study carried out by Neuper et al. [30] explores the influence of different types of visual feedback in the modulation of the EEG signal during the BCI control. Using a video to show a first-person view of an object-directed grasping movement, they were able to found modulation activity in sensorimotor rhythms caused by this real feedback stimuli. They highlight the importance of the amount of information provided by this condition in order to reduce the reactive bands.

Likewise, Ron-Angevin and Diaz-Estrella [34] made a comparison between the screen condition (Graz) and VR, focusing on the BCI's performance (classification rates). They successfully found improvements in the feedback control of the VR condition in untrained subjects. However, they used car navigation as a task, which could be seen as an abstract object because it is expected natural and realistic feedback, such as an arm doing the imaginary task performed by the user. So far, all of the studies cited above have used different feedback stimuli, but none of them has used a virtual arm, which could be useful for the training step.

Precisely, Skola and Liarnokapis [35] carried out a recent work using an embodied VR training for MI-BCI. A human-like avatar performs the motor actions in synchrony with the user's actions. This neurofeedback-guided motor imagery training reports improvements in classification rates in comparison with the Graz paradigm. Even though it was not reached a significant difference, the authors report that ERD in VR subjects is stronger than the control group. Likewise, the same sort of results are reported by Braun et al. [7]. However, in this case, an anthropomorphic robotic hand is used as a visual guide. Also, they found differences between the two conditions in the electrodermal activity and subjective measures.

Both works reported that they were inspired by the RHI. They also include within their discussions, the analysis of sense of ownership, agency, and self-location towards the

non-body object, concepts that are being recently taken into account in BCI research [1, 2]. Although, from the RHI, it is demonstrated that the body transfer illusion can be effetedly used in non-attached limbs in both passive (presence) and active (movement) condition [18], so far, there is not a supernumerary limbs BCI system yet. Bashford and Mehring [4] proposed this possibility with their work. They used imaginary third arm for assessing the ownership and agency of a non-body limb in an imitation BCI (i.e. subjects think that their EEG activity is controlling the arm). Results show that there is independent ownership and control – based on the correct movements observed against the subject movements – of the third arm keeping the sense of ownership of the real hands. These findings suggest the capabilities of human of extrapolating limbs to execute motor actions. However, they did not study the use of this third arm as a control command inside the BCI loop.

The contribution in this paper includes a step towards the developing of a system using MI-BCI for supernumerary limbs by performing a study on the ability to control a third imaginary arm, while comparing the effectiveness of using the conventional arrows and fixation cross as training step (*Graz*) against a first-person view using a human avatar (*Hands*). Both training conditions were performed in a VR environment.

3 Materials and Methods

3.1 Overview

An offline MI-BCI experiment, which uses EEG for recording the data and VR scenarios for presenting the stimulus, was conducted in a reduced noise room. The experiment's aim is to check the feasibility of controlling a virtual third arm using MI-BCI while the traditional training paradigm (Graz) is compared against a first-person view using a human avatar. There were two recording sessions with two runs in each one with a resting time between them. The sessions were conducted on two separate days within one week. Only on the first day, two questionnaires were conducted (MIQ-3 and demographic information). The participants filled up the NASA-TLX form after each session.

3.2 Participants

Ten right-handed volunteers (four women) participated in the study. Participant ages were within 18 and 34 years old with a mean of 23. All participants had basic informatics knowledge. Only 30% did not have previous experience with VR and all of them had any previous experience in MI-BCI. Nobody had problems with the head movements. The half of our population had visual impairments (mainly myopia

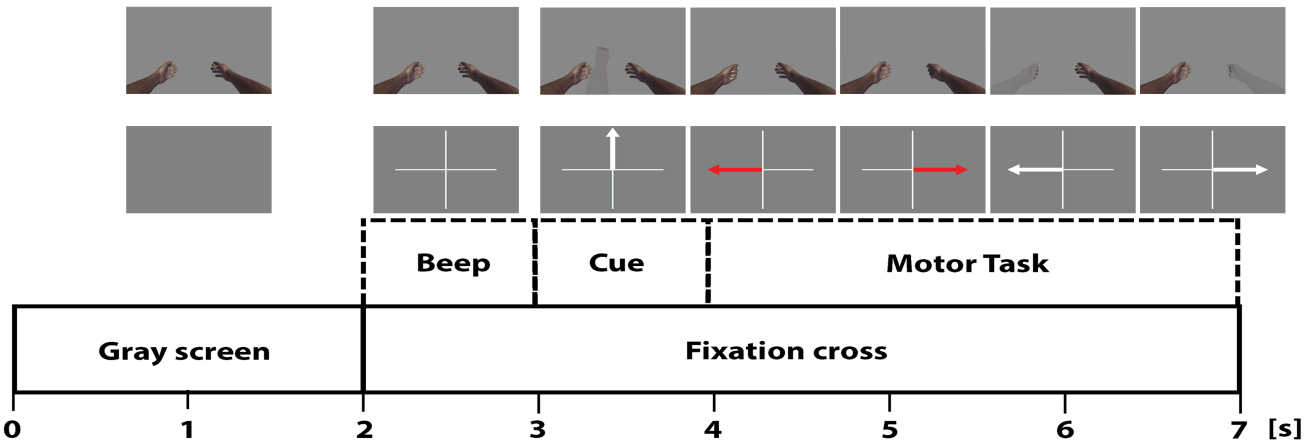


Fig. 2 Experiment paradigm. The visual stimulus of the task's cue are corresponding for both conditions. Top: visual stimuli for *Hands* condition. Middle: visual stimuli for *Graz* condition. Bottom: timing of the trials following the classic Graz protocol.

and astigmatism). The experiment was conducted in accordance with the Declaration of Helsinki. Participants were informed both oral and written about the procedure and the EEG recording. All participants gave written informed consent.

3.3 Apparatus

The EEG data was collected using an OpenBCI 32 bit board at a sampling rate of 250 Hz. Eight passive gold cup electrodes were used and placed at sensorimotor cortex (see Fig. 1 bottom), namely, frontal (F3, Fz, F4), central (C3, Cz, C4), and parietal (P4, P3) cortices, following the 10-20 system. Left and right mastoids were used as reference and ground electrodes respectively.

We used a head-mounted display (HMD) Oculus Rift CV1 with a resolution of 2160 x 1200 (1080 x 1200 per eye), refresh rate of 90 Hz, a 110° field of view, and both rotational and positional tracking for delivery the immersive scene. The popular game engine Unity3D was used to develop the immersive scene that was intended to assist the user when imagining and performing motor actions with their arms, left and right real arms and the middle imaginary one (see Fig. 1 top).

There was a special focus on the realism of the models: left and right hands were placed matching with the rest positions of the real hands. A third hand was placed in the middle of the body, like emerging from the chest trying to avoid visual relations with the left or the right arm. The fingers on the third arm also were modified to be symmetric, since that the thumb in either left and right hand can indicate to which arm it belongs, we decided to remove this from the third arm. In this way we ensure an independent arm and not a copy or extension of the existing arms. High-quality textures were used with shaders designed to highlight generic

skin details. Bones in each finger preserves the average human hand proportions. Labstreaminglayer (LSL) is used for recording and synchronizing the EEG data with the Unity trials through LSL4Unity (a third party software).

3.4 Experimental Procedure

The experiment involves the execution of four different tasks in two experimental conditions. The subjects were invited to rest (RS), or to move a specific hand: third hand (TH), left hand (LH), and right hand (RH). Conditions considered were: *Graz*, and *Hands*. The *Hands* condition involved the presentation of a human-like avatar, whereas *Graz* the presentation of arrows.

The subjects sat comfortably in an armchair and were asked to rest their arms in the armrest and avoid any other movements during the recordings. Initially, the participants wore the HMD for getting into the scene and running several trials for learning the instructions previously read. After the training, we mounted the EEG cap followed by the traditional gelling process, and then we fit the HMD. We tried as much as possible to avoid that the HMD frame touches the EEG electrodes. Moreover, we checked the signal quality before and after mounting the HMD.

The two experimental conditions followed the timing protocol proposed by Pfurtscheller [33]. The users performed 20 trials of each task (randomly selected) with a duration of 7 seconds (see the bottom side of Fig.2). The main difference between the conditions lies in the visual feedback, as follows:

1. *Graz* condition: starting with a gray screen (resting state), at time 2s, a fixation cross at the center of the scene was displayed with a short warning tone ('beep') which indicates to the user to pay attention to the incoming visual

cue presented at time 3s. At time 4s, the user had to perform the motor task for three seconds. The color of the arrows indicates the task (red for execution and white for imagination) and its direction indicates if the hand should be either left or right. The third arm cue was an arrow pointing upwards (see the middle of Fig. 2).

2. *Hands* condition: at the start, the user's hands were placed in the equivalent real arms positions (resting state), at time 2s, the same auditory cue starts indicating an incoming stimulus. Next at time 3s, a visual cue is introduced without animation to let the user prepare for the action they will. At time 4s, the animation is introduced, and the user must perform either the mechanic or imaginary operation. This state continues until the end of the task (three sec more). For the visual cues, the real skin shading represents actual open-close hand movements, while transparent shading represent imaginary movements. Moreover, it is important to highlight that the third arm appears in the scene only when this specific trial is necessary. In other trials, there are just two visible hands (see the top of Fig. 2).

Following [29], subjects were instructed to perform the kinesthetic experience in motor imagery tasks, i.e., imagining the sensation of performing the motor tasks rather than the visual representation of the movement. The authors suggest that kinesthetic motor imagery is essential to elicit sensorimotor patterns (ERD\S). Besides, in order to avoid the carry-over bias, both experimental conditions were counterbalanced across participants (i.e. five subjects start with *Hands* condition and the rest with *Graz*). Likewise, it is necessary to mention that the movement animations were applied directly to the bones always looking for a natural behavior of the hand. The animations are predefined, they are not based on the user's EEG activity.

Finally, in contrast to Skola and Liarnokapis [35] where the *Graz* condition is presented in a monitor, we perform comparisons of the *Graz* and *Hands* conditions in a virtual environment. Therefore, the users have to wear the HMD in both conditions. The background of *Graz* scenario was set to gray, avoiding high contrast that could produce discomfort on the user's eyes.

3.5 EEG signal processing

3.5.1 EEG pre-processing

The recorded data is imported and processed into EEGLAB (14.1) [9] (under Matlab 2017b). After down-sampling at 115hz, the signals are band-pass filtered at range 1-35Hz using a finite impulse response (FIR) filter. Usually, a notch filter is used for line noise, but this method generally creates band-holes, and distortions close the cut-off frequency.

Therefore, the Cleanline plugin, which uses multi-taper regression for removing sinusoidal artifacts, is used at 50-115 Hz instead. Likewise, Cleanraw plugin is set-up for rejecting bad channel. The rejected channels are then interpolated using a spherical function. Finally, EEG signals are re-referenced using common average referenced (CAR).

This study aims to explore as much as possible the influence of both time window of the trials and the frequency bands on the accuracy of the classifiers. Therefore, we used a Filter Bank Common Spatial Patterns (FBCSP) algorithm [3] for several time windows (100, 200, 400, 600, 800, 1000 and 2000 ms) for extracting features and evaluating the classification accuracy. The bank with the MI frequency bands is comprised of alpha (8-12 Hz), low beta (12-16 Hz), middle beta (16-24 Hz), high beta (24-30 Hz), and whole beta (12-30 Hz) bands. The reason of splitting the beta band into sub-bands is for getting enough variables for the FBCSP algorithm to work.

3.5.2 Feature extraction

The ERS/ERD patterns are predominant in alpha (8-12 Hz), and beta (13-30 Hz) rhythms and in its onset goes from 500ms up to three seconds after the movement execution [32]. Inspired by these facts, we built a framework to obtain the best combination of window size, frequency band, and classifier for each user. For obtaining a pool of possible combinations, we ran the Filter Bank Common Spatial Pattern (FBCSP) algorithm [3] in seven time-window sizes of the signal (100, 200, 400, 600, 800, 1000 and 2000 ms)) and five frequency bands (8-12 Hz, 12-16 Hz, 16-24 Hz, 24-30 Hz, 12-30 Hz).

The method employs a greedy algorithm to heuristically find the best combination based on the classification error rates of all possibilities. We focused on the variability that exists across the users in their performance. So, with this approach, we were able to create a suitable and user-centered BCI classification.

The FBCSP approach has demonstrated successful performance in BCI applications [3]. This method extracts the most relevant spectral and spatial features using a CSP filter for each frequency band. CSP is one of the most known and widely used methods for extracting features in a two classes BCI application [5, 21]. CSP computes the project matrix $\mathbf{W} \in \mathbb{R}^{c \times c}$ that linearly transforms the band-pass filtered data $\mathbf{E} \in \mathbb{R}^{c \times t}$ into a spatial filtered signal $\mathbf{Z} \in \mathbb{R}^{c \times t}$ (with c being the number of channels and t the EEG samples per channel) as follows:

$$\mathbf{Z} = \mathbf{W}^T \mathbf{E} \quad (1)$$

Thus, the power of \mathbf{Z} effectively discriminates two mental states (classes), maximizing the variance under one condition meanwhile it is minimizing for the other [5]. In order

to get the most discriminative patterns, the first and last m ($m=3$) columns of \mathbf{W} were used to create the spatial-filtered signal \mathbf{Z} . The m -dimensional feature vector is then formed from the logarithm of the normalized variance of \mathbf{Z} :

$$v_i = \log(\text{var}(Z_i)), \quad i = 1, 2, \dots, 2m. \quad (2)$$

This results in 30 features (six CSP filters per each frequency bands) for each EEG trial in the specific window. From these features, the maximum Relevance Minimum Redundancy (mRMR) feature selection algorithm is used to extract the most relevant features [31]. This algorithm minimizes the redundancy meanwhile maximize the relevance of the features using mutual information. As the size of v_i depends on the frequency bands, the number of selected features was progressively increased (step = 3) from the minimum amount (6) up to the total size of v_i . Hence, the selected features for each time window is used to separately train three common BCI classifiers [22]: Support Vector Machine (SVM), K-Nearest Neighbor (KNN), and Linear Discriminant Analysis (LDA).

3.6 Classification

Linear classifiers have successfully demonstrated their excellent performance in BCI applications due to their simplicity and processing time [22]. Therefore, we used two of the most popular linear approaches (SVM and LDA) and a non-parametric method (KNN). SVM finds the optimal separation hyperplane by maximizing the margin. Meanwhile, LDA obtains the hyperplane by the projection that maximizes the distance between the classes means and minimizes the inter-class variance [22]. Likewise, KNN assigns the class label to the incoming data according to the set of k nearest training data using a metric distance.

These methods were trained to classify independently four binary imaginary tasks: Third and Left hand (TH\RH); Third and Right hand (TH\R); Third hand and Resting State (TH\RS); and Left and Right hand (LH\R). The reader can notice that the real movements are not included in the classification. The intention of including the real movements in the experiment was to reduce the abstractness of the three imaginative tasks and have a fresh mental representation of the action.

The miss-classification error was computed using the usual k-fold cross-validation approach. This method randomly divides the data into k equal size partitions and uses $k-1$ sets to train the model and one set to validate it. In this study, we used ten times the 10-fold cross-validation. Finally, the above classifiers were implemented using the Statistics and Machine Learning Toolbox of Matlab. Both SVM and LDA used the default parameters (linear kernel and standardize predictor data for SVM and LDA without hyperparameter optimization). KNN used a Euclidean distance with $k = 5$.

3.6.1 Event-related spectral perturbation

The event-related spectral perturbation (ERSP) is a generalization of the ERD/ERS patterns. ERSP computes the changes of the spectral powers in time-frequency domains, relative to the stimuli [9]. Thus, with this approach, the changes of the EEG signals elicited by motor imagery events can be clearly detected alongside of the spectral band and epoch. ERSP values were computed for every mental task (TH, LH, RH, RS) in *Graz* and *Hands* conditions using the *newtime* function of the toolbox. A time window of -500 ms to 2500 ms and displayed between 5 Hz and 30 Hz, significant alpha was setup to 0.05. The sensorimotor area composed by the electrodes C3, Cz and C4 were used to display the time-frequency ERD/ERS maps (Figs. 3 and 4).

3.6.2 Task load index

Besides of the subjective assessment of the cognitive load by the NASA-TLX [16], the Task load index developed by Alan Gevins and Michael E. Smith [36] is used in order to have an objective measure of the task load. The authors found that the power changes of θ at frontal mid-line sites and α at parietal sites are related to the task load associated to the mental effort required for task performance. Thus, this index can be measured by the ratio of θ to α . In this work, the average of the absolute power of frontal mid-line (F3, Fz, F4) θ and parietal (P3-P4 plus Cz) α were used to assess the mental tasks per condition (*Graz* and *Hands*).

4 Results

4.1 ERD/ERS results

Figures 3 and 4 show the time-frequency representation of significant (bootstrap method, $p < 0.05$) ERD/ERS values (blue indicates ERD) for the *Hands* and *Graz* condition respectively. These maps coming from a single subject (6) at electrode positions C3, Cz and C4.

For the TH task, at C3 position in *Hands* condition, a strong power decrease is clearly visible around 500ms after stimulus onset, and this behavior is presented in almost the whole frequency range; whereas in the other two imagery tasks, LH has a decrease in alpha followed by an increase in alpha and beta; RH has a similar pattern but without an ERS activity in alpha. Interestingly, TH task held the ERD activity during the rest of the epoch after 1000ms with few ERS in middle and high beta band. Conversely, in *Graz* condition at C3, the ERS patterns of the TH task are attenuated and widespread with some ERS activity at the end of the epoch in high beta band.

At Cz in *Hands* condition, the TH task presents an ERD activity that starts around 500ms in alpha, and an ERS that

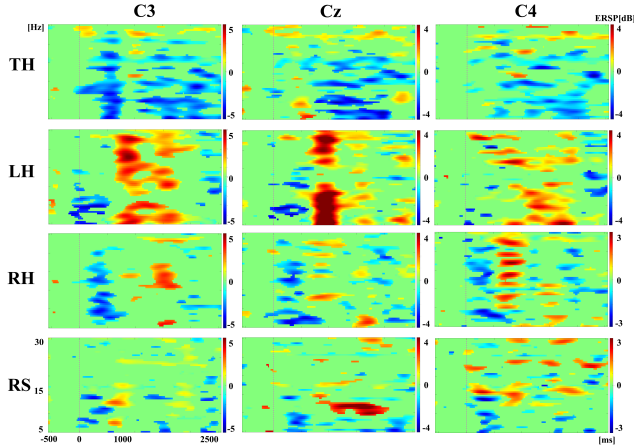


Fig. 3 Significant ERD/ERS patterns of the mental task at C3, Cz, C4 positions for Hands condition. A strong ERD activity is found at the three electrodes for the third hand (TH). Whereas, ERS patterns are found mainly for the left hand (LH). The ERD/ERS fluctuation is more visible for the right hand (RH), mostly at C4.

starts around 1000ms in alpha and beta band. LH presents a strong ERD activity in both alpha and beta anticipated by an ERS in alpha and middle beta. RH has a strong ERD activity in alpha and beta and posteriorly some ERS in beta. Meanwhile, in Graz condition, TH shows ERS pattern in beta along with the first 500ms and followed by an ERD in alpha. At the end of the epoch, some ERS activity is presented in high beta. In LH, there is an ERD pattern is presented in alpha during the first 500ms and a widespread ERS activity later. RH holds the ERD in alpha at the same time with some ERS middle beta.

Similarly, TH task in Hands condition presents an ERD pattern around 500ms in alpha and middle beta at the C4 position. This activity is held again during the epoch. Some ERS activity is found in high beta after 1000ms. The ERS activity is most prominent in alpha and low-middle beta for LH, meanwhile, RH shows a common ERD/ERS pattern in alpha and beta in the first 1000ms. For Graz condition, the ERD patterns of TH task are widespread in alpha and beta between 500ms and 1500ms with some presence of ERS in high beta. LH has a strong ERD activity during the first 1000ms in alpha and some widespread ERS in high beta. RH has strong ERD patterns during the same previous time in both alpha and middle beta followed by a strong ERS activity in alpha, extended along of the epoch.

In order to explore the differences of the ERD/ERS patterns among tasks in the two conditions, Figure 5 shows a comparison of the power changes of the TH task against the other imagery tasks (LH/RH) in both conditions using the same electrodes array. The paired Wilcoxon signed-rank test was used to find out significant differences between tasks ($p < 0.05$). They are shaded by gray blocks. Blue and red lines represent Hands condition meanwhile Graz condition with

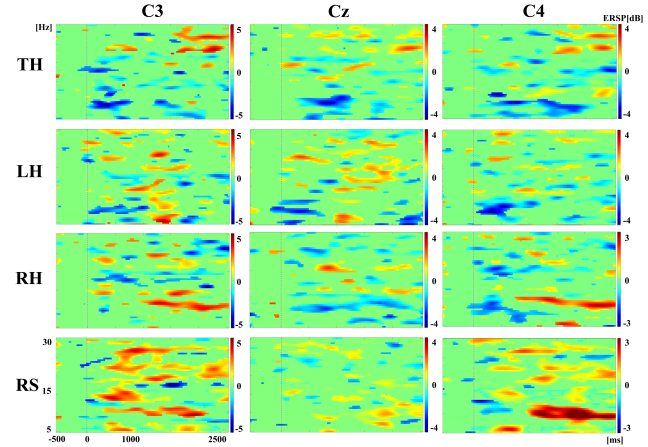


Fig. 4 Significant ERD/ERS patterns of the mental task at C3, Cz, C4 positions for Graz condition. An ERD activity is mainly found in the alpha band (8-12 Hz) at the three electrodes for the third hand (TH). The ERD/ERS patterns are widespread for left and right hands (LH, RH respectively) at the three electrodes. There is extensive activity in the resting state (RS).

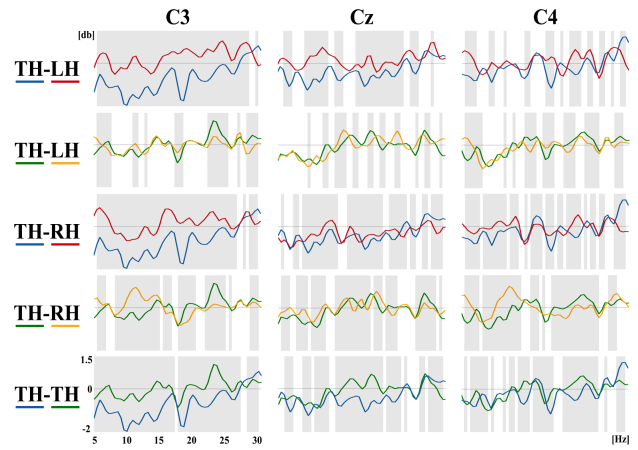


Fig. 5 Comparison of the power changes of the mental tasks in the sensory-motor area (C3, Cz, C4). Gray areas denotes significant differences. Blue and red lines represent the tasks in Hands condition, whereas green and yellow in Graz condition.

green and orange lines. Furthermore, the bottom part of the plot shows a comparison of TH signal in Hands (blue) and Graz (green) conditions.

The differences presented by TH-LH and TH-RH are significantly more broad-banded at C3 than the other channels in hands condition. Meanwhile, Graz condition presents similar significant region sizes among the channels. At C3, both groups of Hands condition show significant differences in almost the whole frequency range. Conversely, in Graz condition, TH-RH shows more significant differences in alpha and low beta than TH-LH, but they share the significant region around 20Hz up to 25Hz. At Cz in Hands, the TH-LH comparison does not have a significant region in the alpha band, but it shares a low and middle beta with TH-

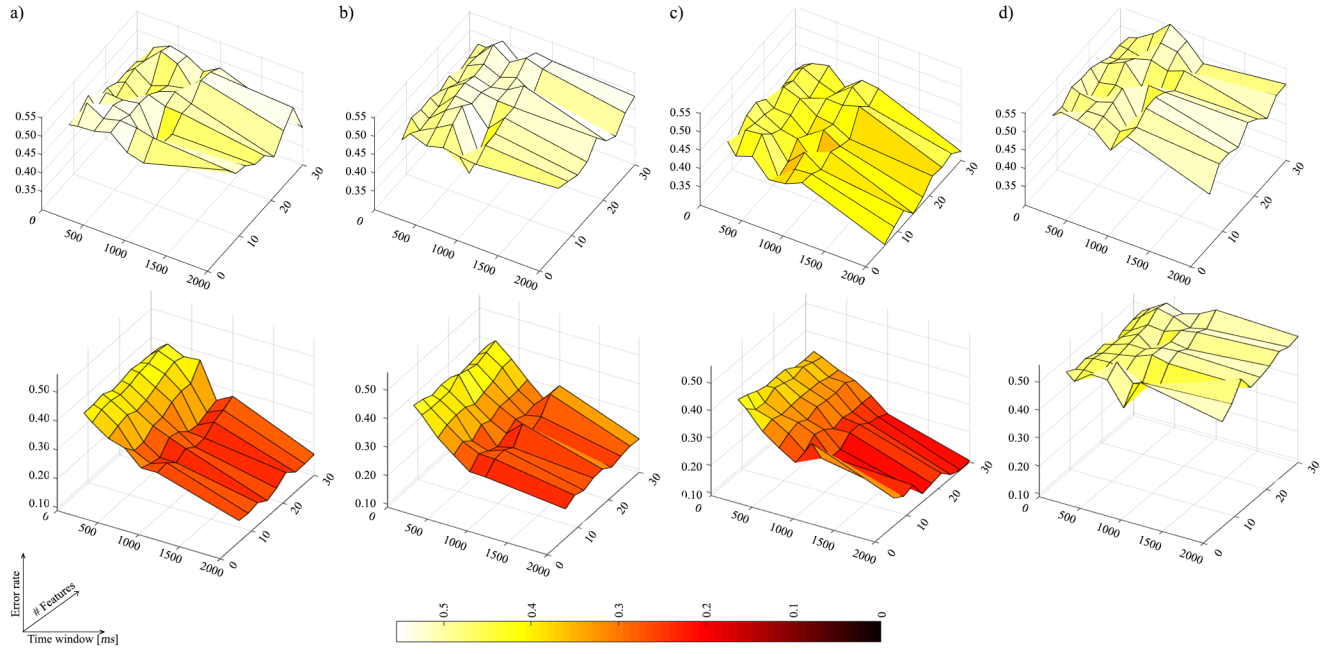


Fig. 6 Error rates over number of features and time window size for all users. Top: Graz condition. Bottom: Hands condition. The four binary classification are represented by a)TH/LH; b)TH/RH; c)TH/RS; and d)LH/RH.

RH, which has significant differences in some alpha and high beta sub-bands. For Graz, the TH-LH comparison indicates wide-spread sub-band regions for the beta, in alpha only a small region around 10hz is presented and, meantime, TH-RH shows a consistent region in alpha and low and high beta. Finally, at C4 in Hands, the TH-RH comparison shows more wide regions than TH-LH, especially in alpha and middle beta rhythms. The same behavior is presented in Graz condition, where TH-RH has more significant regions in alpha and low and middle beta than TH-LH, which does not have a significant difference in alpha, only in several sub-bands along beta, mainly upper than 15Hz.

In the comparison of the TH task between conditions, the ERS patterns are stronger in Hands than Graz (in line with the maps). This difference is more evident at C3 than the other channels. Likewise, C3 noticeably shows significant regions within both alpha and beta rhythms, whereas Cz is more often in middle and high beta, and C4 in alpha and middle beta.

4.2 Classification results

The Fig 6 shows the error rates in function of the number of features and the size of the time windows for the KNN in each binary classification. We obtained these surfaces for both Graz (top) and Hands (bottom) conditions as well as for each classifier (SVM, KNN, LDA). Initially, we can see that Hands condition reached lower error rates than Graz for KNN. Likewise, the error rates are better in the classification

that includes the third arm (a), b), c) in the Fig 6) than the left and right classification (d) in the Fig 6); in effect, the RH/LH classification reached error rates close to 0.5, which means a classification by chance. Finally, the tendency in both conditions is that as the size of the time window increases the error rates decrease but in the number of features the tendency is unclear.

Following the error mean values of each window\feature, we built a greedy algorithm to find the optimal global choice. Thus, we can obtain for each subject, the best combination of the three conditions (i.e. number of features (NF), size of the window (SW) and classifier (C)) to get the best miss classification rate (error). The table 1 shows these values in Graz (G) and Hands (H) conditions among the subjects.

We merged the data of each run into a single dataset for thus training the classifiers. The table shows that there are several variations across the subjects and conditions. Only in TH\RS task, the number of features was widespread. Otherwise, the distribution was concentrated from six up to 21, precisely, the fig 7 shows the histogram of selection of each frequency component over all subjects for the four binary classifications. In the figure can be seen that frequency components in the alpha and beta3 were selected for most of the participants, in effect, the clear peaks are inside these ranges. Meanwhile, the whole beta band (beta 4) was few used, showing how the beta sub-bands can be used more than the whole band itself. In the other side, for the size of the time window, the classification that includes the third arm (TH-RH,TH-LH and TH-RS) was superior of the 800ms up to

Table 1 The best combinations of number of features, time window and classifier and the error rates reached with them across the subjects for both conditions. The asterisks indicate the subjects that began the experiment with the Hands condition.

Subject	Condition	TH-RH				TH-LH				TH-RS				LH-RH			
		NF	SW	C	Error	NF	SW	C	Error	NF	SW	C	Error	NF	SW	C	Error
1*	G	6	2000	KNN	0.18	6	2000	KNN	0.18	6	800	LDA	0.24	9	2000	LDA	0.42
	H	9	2000	LDA	0.17	12	2000	KNN	0.28	15	1000	SVM	0.27	12	2000	SVM	0.41
2	G	6	800	SVM	0.26	24	100	KNN	0.40	9	2000	SVM	0.16	6	2000	KNN	0.30
	H	6	2000	KNN	0.19	6	2000	LDA	0.13	24	2000	SVM	0.24	21	800	KNN	0.39
3	G	6	800	LDA	0.42	6	800	KNN	0.41	12	2000	KNN	0.35	21	600	KNN	0.45
	H	12	1000	SVM	0.40	9	2000	KNN	0.34	12	2000	KNN	0.27	6	100	KNN	0.48
4*	G	30	100	KNN	0.42	6	800	LDA	0.41	24	1000	KNN	0.37	6	100	SVM	0.46
	H	15	100	KNN	0.47	6	400	LDA	0.45	18	600	KNN	0.37	6	1000	SVM	0.36
5	G	30	800	SVM	0.31	6	100	LDA	0.46	12	600	KNN	0.28	15	100	KNN	0.45
	H	12	2000	KNN	0.34	24	800	SVM	0.41	15	400	KNN	0.42	12	2000	KNN	0.38
6*	G	21	2000	KNN	0.40	6	100	LDA	0.42	18	2000	SVM	0.26	6	800	KNN	0.45
	H	18	2000	SVM	0.10	6	2000	SVM	0.16	30	2000	KNN	0.09	21	400	SVM	0.42
7	G	15	2000	SVM	0.38	18	800	SVM	0.38	21	400	SVM	0.37	21	2000	KNN	0.41
	H	21	200	LDA	0.28	30	1000	KNN	0.38	9	1000	SVM	0.34	6	800	SVM	0.44
8*	G	6	800	LDA	0.36	9	800	SVM	0.40	18	2000	SVM	0.31	6	200	SVM	0.46
	H	9	800	SVM	0.39	12	800	LDA	0.41	6	800	LDA	0.35	21	800	LDA	0.37
9	G	12	800	KNN	0.38	6	100	SVM	0.48	27	2000	KNN	0.34	15	600	LDA	0.40
	H	21	1000	KNN	0.31	9	1000	SVM	0.22	27	800	KNN	0.37	9	800	LDA	0.37
10*	G	12	800	KNN	0.32	9	800	LDA	0.34	6	2000	KNN	0.22	6	100	SVM	0.46
	H	6	800	SVM	0.25	6	2000	KNN	0.21	9	2000	LDA	0.22	6	2000	SVM	0.36

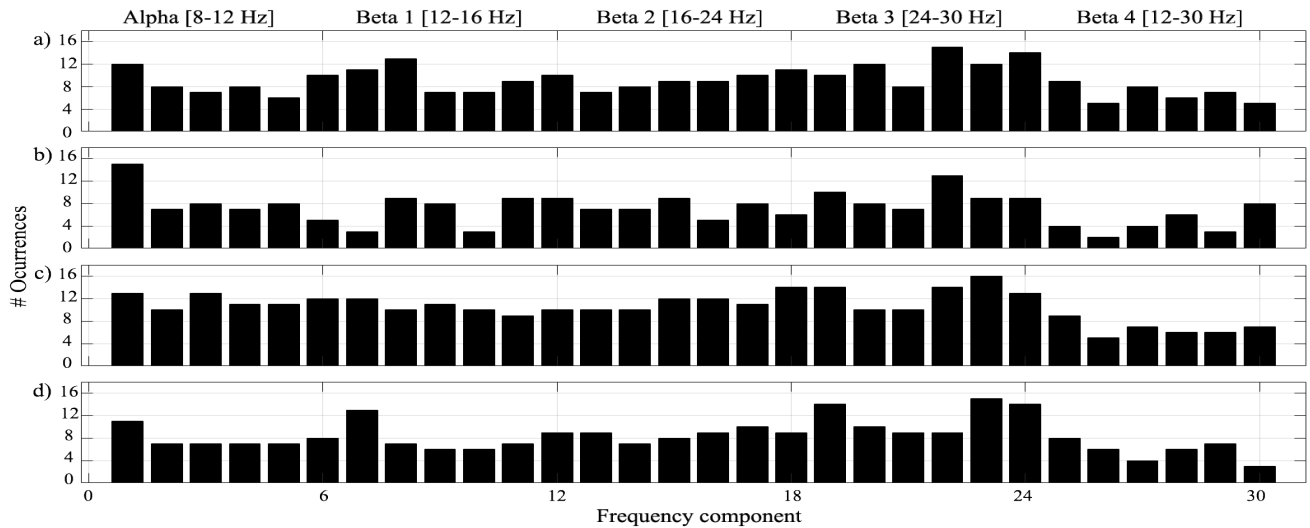


Fig. 7 Relevant frequency components over all subjects. a) TH\RH; b) TH\RH; c) TH\RS; d) LH\RH.

2sec (maximum time). Finally, the KNN was the most used among the participants and conditions.

The mean error obtained over all participants ($n=10$) in Hands condition was approx 32% (i.e. TH-LH: 0.29 ± 0.03 , TH-RH: 0.29 ± 0.03 , TH-RS: 0.29 ± 0.03 , and LH-RH: 0.39 ± 0.01) and around 36% in Graz condition (i.e. TH-LH: 0.34 ± 0.02 , TH-RH: 0.38 ± 0.02 , TH-RS: 0.29 ± 0.02 , and LH-RH: 0.42 ± 0.01). Pairwise comparison using paired Wilcoxon signed rank test with Bonferroni correction reveals a significant ($V = 0$, p -value = 0.048) between conditions. Likewise, Dunn's Kruskal-Wallis Multiple Comparisons with Bonferroni correction show significant difference among groups, exactly in both TH-LH ($z=-2.49$, p -value=0.03) and TH-RS ($z=-3.92$, p -value=0.0003) against LH-RH for Graz, and in Hands only for TH-RS ($z=-2.44$, p -value=0.04).

In summary, the Hands condition significantly outperforms (0.32) the Graz (0.36) in the classification. Intriguingly, the classification of TH-LH was better than the other two motor imagery condition (TH-RH, LH-RH) in both conditions (Graz = 0.34, Hands=0.29).

4.3 Cognitive load results

Figure 8 shows the cognitive load of both objective (Task Load Index) and subjective (NASA-TLX). The cognitive load assessed by the Task Load Index reflects the fact of that Hands condition has a significantly higher cognitive load than the Graz (pairwise paired Wilcox with Bonferroni: $V = 656$, p -value = 0.00063). There is no significant differ-

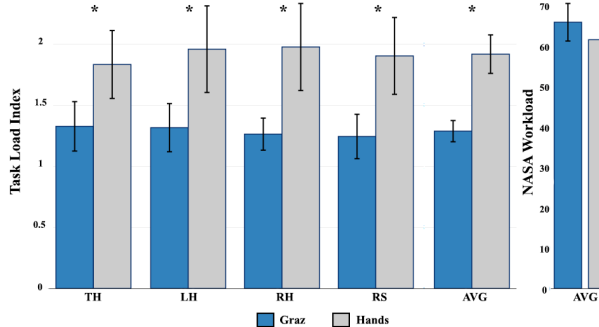


Fig. 8 Task Load Index and NASA Workload for the two conditions.

* Significant differences

ence among task. Meanwhile, the subjective assessment of the cognitive load reflects the opposite; the NASA Workload points to a higher cognitive load in Graz condition than in Hands although significance could not be found (paired t-test: $t=0.829$, $p\text{-value}=0.428$). Nevertheless, a pairwise paired Wilcoxon reflects that there is a significant difference between conditions in the Frustration factor ($V=210$, $p\text{-value}=0.049$), indicating a higher sense of frustration in Graz than Hands condition. Figure 9 shows that Hand condition presents a non-significant higher Load Magnitude than Graz in factors such as Performance, Physical and Temporal demand.

4.4 Other results

On the other hand, we used Spearman's rank correlation in order to find out any relationship between the classification error and both the questionnaires (NASA-TLX and MIQ-3) and the Task Load Index. There are no any significant correlations in both MIQ-3 and Task Load Index with the performance of the users. Meanwhile, in the NASA-TLX, there is a significant correlation ($\rho=-0.366$, $p\text{-value}=0.019$) in Mental demand factor for the Hand condition. Inside this condition, only the TH-LH classification has a significant correlation with this factor ($\rho=-0.693$, $p\text{-value}=0.0261$).

5 Discussion

This study proposed the inclusion of a third arm in an MI-BCI application creating thus a supernumerary limb MI-BCI system. Furthermore, for this approach, the influence of embodiment feedback (*Hands*) was compared with the standard Graz training in VR. Evidently, and in line with the previous works [7, 35], both the classification rates and the modulation of ERS signals were enhanced by the realistic feedback, evidencing its importance inside the BCI loop. Also, our work goes further than the one done by Skola and Liarnokapis [35] because they compared the embodiment VR scenario against the monitor-based Graz, creating

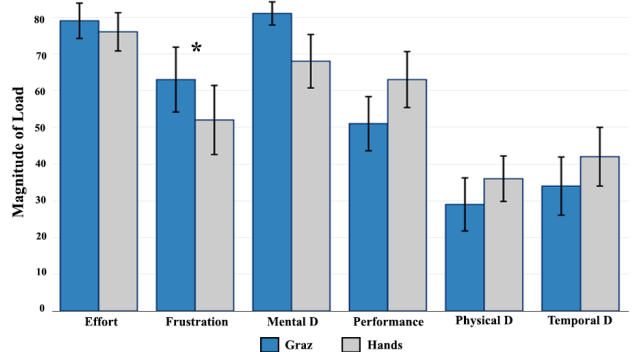


Fig. 9 NASA factors for the two conditions. *Significant difference.

a bias in the users who started with the VR. Here, the comparison was made with both Graz and Hands experimental conditions made in VR.

The high error rates presented by the left-right hand classification (LH/RH) in both conditions (Hands: 0.39 ± 0.01 , Graz: 0.42 ± 0.01) could suggest that the inclusion of the third arm would cause the reduction of its accuracy because the users could interpret either left and right hand as the third arm. Whereas, the third arm is distinguished from the left hand than the right with better accuracies. It could support the fact that the TH task follows the activity based on the handedness. Unfortunately, all of our subjects were right-handed, so we can not evaluate the handedness thoroughly in this experiment.

The presented patterns (figures 3 and 4) suggest a significant decreasing activity in the sensorimotor area caused by realistic feedback in comparison with the Graz. Besides, the ERD activity of TH task is prominent at the three sensorimotor channels (C3, Cz C4) which could suggest that there is not a compulsory hemisphere governing the control and action of the imaginary arm. Nevertheless, the analysis of the power changes between tasks (figure 5) shows that there are more significant regions at C3 than the other electrode positions. The fact above could indicate that the user's handedness influences the region where TH task presents more activity. In the same way, the common ERD/ERS pattern is visible in LH and RH tasks, more in RH than LH, but it was missed in TH (only an increasing power activity was found in high frequencies: $> 25\text{Hz}$). It suggests that the absence of symmetry of the third arm does not elicit a supplementary ERS activity for this task.

Intriguingly, the decreasing activity of TH is widespread along of the epoch in several frequency rhythms, keeping its strength. That is visible at the three electrode positions in Hand condition (more at C3). This fact motivates to the authors to adopt several time windows and frequency bands in order to obtain the most suitable combination for classification (see EEG signal processing section). Moreover, the unexpected activities presented in the resting state (RS) could

be caused by the inertia of the motor/imagery movement. The paradigm to be adopted in the future should include a blank space between the motor task and resting state so that the movements could be easily excluded.

The aim of studying the cognitive load in both subjective and objective ways is for a deeper understanding of the additional load that realistic and visual feedback could cause. In effect, the outcome of the objective assessment (Task Load Index) goes against to the results of the subjective one (NASA-TLX). EEG data reveals that the cognitive load is higher (significantly) in the realistic condition (Hands) than the standard one (Graz) but the opposite is presented in the NASA-TLX (without significance). Moreover, some user's comments at the end of the experiment, such as "I found harder the arrows than the arms" or "I feel Temporal demand a bit easier in Hands than Graz because it is easier to visualize" and the opposite "... The arrow session was a less hard than the virtual hands because with the arms I constantly tried to follow the hand movements which did not happen with the arrows" could evidence the disjunctive sensation of the users evidenced by the NASA and Task Load Index. Interestingly, a user did the next comment "The fact that I had the possibility of performing real hand movement helped me to release the stress created by the imagery tasks" This comment supports the intention of keeping the real movements but further studies and comparisons are necessary before drawing conclusions.

6 Conclusions

This study investigated the possibility of using an imaginary third arm and the differences of the EEG patterns and classification rates of using a realistic visual feedback. In line with the discussion above, the visual processing plays a vital role in the task load. Despite that the Hands condition was kept as simple as possible, it could not be possible to maintain a low cognitive load like in Graz, in effect, the processing of visual animation is higher than arrows and fixation cross. However, the benefits presented by this feedback are reflected in the enhanced of the ERS signals that consequently produces an improvement of the classification. Supernumerary MI-BCI systems are prominent and possible uses should be explored, especially for VR applications, where customized avatars could be controlled using imaginary non-body signals.

Unfortunately, this work lacks in studies about ownership of the third-arm in both subjectively, with questions about the sense of agency and sense of ownership, and objectively, using galvanic skin response (GSR), following the work of Bashford and Mehring [4]. These data could give some insights regarding the use of supernumerary BCI and how it could be used in real application, coming from the answers of the users. Also, it would be necessary to perform

the experiment with left-handed people, in order to study the handiness of the third arm.

References

1. Alimardani, M., Nishio, S., Ishiguro, H.: Effect of biased feedback on motor imagery learning in bci-teleoperation system. *Frontiers in Systems Neuroscience* **8**, 52 (2014). DOI 10.3389/fnsys.2014.00052
2. Alimardani, M., Nishio, S., Ishiguro, H.: Removal of proprioception by bci raises a stronger body ownership illusion in control of a humanlike robot. *Scientific Reports* **6**, 33,514 EP – (2016). DOI <https://doi.org/10.1038/srep33514>. Article
3. Ang, K.K., Chin, Z.Y., Zhang, H., Guan, C.: Filter bank common spatial pattern (fbcsp) in brain-computer interface. In: 2008 IEEE International Joint Conference on Neural Networks (IEEE World Congress on Computational Intelligence), pp. 2390–2397 (2008). DOI 10.1109/IJCNN.2008.4634130
4. Bashford, L., Mehring, C.: Ownership and agency of an independent supernumerary hand induced by an imitation brain-computer interface. *PLOS ONE* **11**(6), 1–15 (2016). DOI 10.1371/journal.pone.0156591
5. Blankertz, B., Tomioka, R., Lemm, S., Kawanabe, M., Muller, K.: Optimizing spatial filters for robust eeg single-trial analysis. *IEEE Signal Processing Magazine* **25**(1), 41–56 (2008). DOI 10.1109/MSP.2008.4408441
6. Botvinick, M., Cohen, J.: Rubber hands feel touch that eyes see. *Nature* **391**, 756 EP – (1998)
7. Braun, N., Emkes, R., Thorne, J.D., Debener, S.: Embodied neurofeedback with an anthropomorphic robotic hand. *Scientific Reports* **6**, 37,696 EP – (2016). DOI <https://doi.org/10.1038/srep37696>. Article
8. Chavarriaga, R., Fried-Oken, M., Kleih, S., Lotte, F., Scherer, R.: Heading for new shores! overcoming pitfalls in bci design. *Brain Computer Interfaces* (Abingdon, England) **4**(1-2), 60–73 (2017). DOI 10.1080/2326263X.2016.1263916
9. Delorme, A., Makeig, S.: Eeglab: an open source toolbox for analysis of single-trial eeg dynamics including independent component analysis. *Journal of Neuroscience Methods* **134**(1), 9 – 21 (2004). DOI <https://doi.org/10.1016/j.jneumeth.2003.10.009>
10. Donalek, C., Djorgovski, S.G., Cioc, A., Wang, A., Zhang, J., Lawler, E., Yeh, S., Mahabal, A., Graham, M., Drake, A., Davidoff, S., Norris, J.S., Longo, G.: Immersive and collaborative data visualization using virtual reality platforms. In: 2014 IEEE International Conference on Big Data (Big Data), pp. 609–614 (2014). DOI 10.1109/BigData.2014.7004282
11. Donchin, E., Spencer, K.M., Wijesinghe, R.: The mental prosthesis: assessing the speed of a p300-based brain-computer interface. *IEEE Transactions on Rehabilitation Engineering* **8**(2), 174–179 (2000). DOI 10.1109/86.847808
12. Ferri, F., Chiarelli, A.M., Merla, A., Gallesio, V., Costantini, M.: The body beyond the body: expectation of a sensory event is enough to induce ownership over a fake hand. *Proceedings of the Royal Society B: Biological Sciences* **280**(1765), 20131,140 (2013). DOI 10.1098/rspb.2013.1140
13. Gamito, P., Oliveira, J., Coelho, C., Morais, D., Lopes, P., Pacheco, J., Brito, R., Soares, F., Santos, N., Barata, A.F.: Cognitive training on stroke patients via virtual reality-based serious games. *Disability and Rehabilitation* **39**(4), 385–388 (2017). DOI 10.3109/09638288.2014.934925
14. Gert, P., Leeb, R., Faller, J., Neuper, C.: Brain-computer interface systems used for virtual reality control. In: J.J. Kim (ed.) *Virtual Reality*, chap. 7, pp. 1–19. InTech (2011)
15. HA, A.: Virtual reality programs applications in healthcare. *Health Med Informat* **9**, 305 (2018). DOI 10.4172/2157-7420.1000305

16. Hart, S.G., Stavenland, L.E.: Development of NASA-TLX (Task Load Index): Results of empirical and theoretical research. In: P.A. Hancock, N. Meshkati (eds.) *Human Mental Workload*, chap. 7, pp. 139–183. Elsevier (1988)
17. Jeannerod, M.: Mental imagery in the motor context. *Neuropsychologia* **33**(11), 1419 – 1432 (1995). DOI [https://doi.org/10.1016/0028-3932\(95\)00073-C](https://doi.org/10.1016/0028-3932(95)00073-C). The Neuropsychology of Mental Imagery
18. Kalckert, A., Ehrsson, H.: Moving a rubber hand that feels like your own: A dissociation of ownership and agency. *Frontiers in Human Neuroscience* **6**, 40 (2012). DOI [10.3389/fnhum.2012.00040](https://doi.org/10.3389/fnhum.2012.00040)
19. Lalor, E.C., Kelly, S.P., Finucane, C., Burke, R., Smith, R., Reilly, R.B., McDarby, G.: Steady-state vep-based brain-computer interface control in an immersive 3d gaming environment. *EURASIP Journal on Advances in Signal Processing* **2005**(19), 706,906 (2005). DOI [10.1155/ASP.2005.3156](https://doi.org/10.1155/ASP.2005.3156)
20. Leeb, R., Friedman, D., Müller-Putz, G.R., Scherer, R., Slater, M., Pfurtscheller, G.: Self-paced (asynchronous) bci control of a wheelchair in virtual environments: A case study with a tetraplegic. *Computational Intelligence and Neuroscience* **79642** (2007). DOI [10.1155/2007/79642](https://doi.org/10.1155/2007/79642)
21. Lotte, F.: A Tutorial on EEG Signal Processing Techniques for Mental State Recognition in Brain-Computer Interfaces. In: E.R. Miranda, J. Castet (eds.) *Guide to Brain-Computer Music Interfacing*. Springer (2014). URL <https://hal.inria.fr/hal-01055103>
22. Lotte, F., Bougrain, L., Cichocki, A., Clerc, M., Congedo, M., Rakotomamonjy, A., Yger, F.: A review of classification algorithms for eeg-based braincomputer interfaces: a 10 year update. *Journal of Neural Engineering* **15**(3), 031,005 (2018)
23. Lotte, F., Faller, J., Guger, C., Renard, Y., Pfurtscheller, G., Lécuyer, A., Leeb, R.: Combining BCI with Virtual Reality: Towards New Applications and Improved BCI. In: B.Z. Allison, S. Dunne, R. Leeb, J.D.R. Millán, A. Nijholt (eds.) *Towards Practical Brain-Computer Interfaces*. Springer (2013)
24. Lotte, F., Renard, Y., Lécuyer, A.: Self-Paced Brain-Computer Interaction with Virtual Worlds: A Quantitative and Qualitative Study “Out of the Lab”. In: 4th international Brain Computer Interface Workshop and Training Course. Graz University of Technology, Graz, Austria (2008)
25. Lécuyer, A., Lotte, F., Reilly, R.B., Leeb, R., Hirose, M., Slater, M.: Brain-computer interfaces, virtual reality, and videogames. *Computer* **41**(10), 66–72 (2008). DOI [10.1109/MC.2008.410](https://doi.org/10.1109/MC.2008.410)
26. Mendes, P., A. Marinho, D., Petrica, J., Silveira, P., Monteiro, D., Cid, L.: Translation and validation of the movement imagery questionnaire 3 (miq - 3) with portuguese athletes. *Motricidade* **12**, 149 (2016). DOI [10.6063/motricidade.7006](https://doi.org/10.6063/motricidade.7006)
27. Neuper, C., Müller, G., Kubler, A., Birbaumer, N., Pfurtscheller, G.: Clinical application of an eeg-based brain-computer interface: a case study in a patient with severe motor impairment. *Clinical Neurophysiology* **114**(3), 399 – 409 (2003). DOI [https://doi.org/10.1016/S1388-2457\(02\)00387-5](https://doi.org/10.1016/S1388-2457(02)00387-5)
28. Neuper, C., Pfurtscheller, G.: Neurofeedback Training for BCI Control, pp. 65–78. Springer Berlin Heidelberg, Berlin, Heidelberg (2010)
29. Neuper, C., Scherer, R., Reiner, M., Pfurtscheller, G.: Imagery of motor actions: Differential effects of kinesthetic and visualmotor mode of imagery in single-trial eeg. *Cognitive Brain Research* **25**(3), 668 – 677 (2005). DOI <https://doi.org/10.1016/j.cogbrainres.2005.08.014>
30. Neuper, C., Scherer, R., Wriessnegger, S., Pfurtscheller, G.: Motor imagery and action observation: Modulation of sensorimotor brain rhythms during mental control of a brain-computer interface. *Clinical Neurophysiology* **120**(2), 239 – 247 (2009). DOI <https://doi.org/10.1016/j.clinph.2008.11.015>
31. Peng, H., Long, F., Ding, C.: Feature selection based on mutual information criteria of max-dependency, max-relevance, and min-redundancy. *IEEE Transactions on Pattern Analysis and Machine Intelligence* **27**(8), 1226–1238 (2005). DOI [10.1109/TPAMI.2005.159](https://doi.org/10.1109/TPAMI.2005.159)
32. Pfurtscheller, G.: Quantification of ERD and ERS in the time domain, revised edition vol. 6 edn., pp. 89–105. Elsevier B.V., Netherlands (1999)
33. Pfurtscheller, G., Neuper, C.: Motor imagery and direct brain-computer communication. *Proceedings of the IEEE* **89**(7), 1123–1134 (2001). DOI [10.1109/5.939829](https://doi.org/10.1109/5.939829)
34. Ron-Angevin, R., Diaz-Estrella, A.: Brain-computer interface: Changes in performance using virtual reality techniques. *Neuroscience Letters* **449**(2), 123 – 127 (2009). DOI <https://doi.org/10.1016/j.neulet.2008.10.099>
35. Skola, F., Liarokapis, F.: Embodied vr environment facilitates motor-imagery brain-computer interface training. *Computers and Graphics* **75**, 59 – 71 (2018). DOI <https://doi.org/10.1016/j.cag.2018.05.024>
36. Smith, M.E., Gevins, A., Brown, H., Karnik, A., Du, R.: Monitoring task loading with multivariate eeg measures during complex forms of human-computer interaction. *Human Factors* **43**(3), 366–380 (2001). DOI [10.1518/001872001775898287](https://doi.org/10.1518/001872001775898287)
37. Wolpaw, J.R., Birbaumer, N., McFarland, D.J., Pfurtscheller, G., Vaughan, T.M.: Braincomputer interfaces for communication and control. *Clinical Neurophysiology* **113**(6), 767 – 791 (2002). DOI [https://doi.org/10.1016/S1388-2457\(02\)00057-3](https://doi.org/10.1016/S1388-2457(02)00057-3)
38. Zander, T.O., Gaertner, M., Kothe, C., Vilimek, R.: Combining eye gaze input with a braincomputer interface for touchless humancomputer interaction. *International Journal of HumanComputer Interaction* **27**(1), 38–51 (2010). DOI [10.1080/10447318.2011.535752](https://doi.org/10.1080/10447318.2011.535752)
39. Zander, T.O., Kothe, C.: Towards passive braincomputer interfaces: applying braincomputer interface technology to humanmachine systems in general. *Journal of Neural Engineering* **8**(2), 025,005 (2011)
40. Zander, T.O., Kothe, C., Jatzev, S., Gaertner, M.: Enhancing Human-Computer Interaction withInput from Active and Passive Brain-Computer Interfaces, pp. 181–199. Springer London, London (2010)